Calcium binding and translocation by the voltage-dependent anion channel: a possible regulatory mechanism in mitochondrial function

Dan GINCEL, Hilal ZAID and Varda SHOSHAN-BARMATZ[1]

Department of Life Sciences and Zlotowski Center for Neuroscience, Ben Gurion University of the Negev, Beer Sheva, P.O.B. 653, 84105 Israel

Mitochondria play a central role in energy metabolism, Ca^{2+} signalling, aging and cell death. To control cytosolic or mitochondrial Ca^{2+} concentration, mitochondria possess several Ca^{2+}-transport systems across the inner membrane. However, the pathway for Ca^{2+} crossing the outer membrane has not been directly addressed. We report that purified voltage-dependent anion channel (VDAC) reconstituted into lipid bilayers or liposomes is highly permeable to Ca^{2+}. VDAC contains Ca^{2+}-binding sites that bind Ruthenium Red (RuR), La^{3+} and that RuR completely closed VDACs in single or multichannel experiments. Energized, freshly prepared mitochondria accumulate Ca^{2+} (500–700 nmol/mg of protein), and subsequently released it. The release of Ca^{2+} is accompanied by cyclosporin A-inhibited swelling, suggesting activation of permeability transition pore (PTP). RuR and ruthenium amine binuclear complex, when added to mitochondria after Ca^{2+} accumulation has reached a maximal level and before PTP is activated, prevented the release of Ca^{2+} and the accompanied mitochondrial swelling. RuR also prevented PTP opening promoted by atractyloside, an adenine nucleotide translocase inhibitor. These results suggest that VDAC, located in the mitochondrial outer membrane, controls Ca^{2+} transport into and from the mitochondria, and that the inhibition of Ca^{2+} uptake by RuR and La^{3+} may result from their interaction with VDAC Ca^{2+}-binding sites. Inhibition of PTP opening or assembly by RuR and ruthenium amine binuclear complex suggest the involvement of VDAC in PTP activity and/or regulation. The permeability of VDAC to Ca^{2+} and its binding of Ca^{2+}, suggest that VDAC has a role in regulation of the mitochondrial Ca^{2+} homoeostasis.

Key words: apoptosis, calcium transport, single channel.

INTRODUCTION

Mitochondria, the engines of ATP production, also sequester Ca^{2+} at the expense of energy [1]. Intramitochondrial Ca^{2+} is a major modulator of Ca^{2+}-sensitive metabolic reactions such as those of critical enzymes of the tricarboxylic acid cycle, fatty acid oxidation or amino acid catabolism [2]. Furthermore, mitochondria also function in modulation of cytosolic Ca^{2+} transients [1]. Mitochondrial Ca^{2+} overload is a critical event in both apoptotic and necrotic cell death [3,4]. Mitochondria respond to the apoptotic Ca^{2+} signal by opening the mitochondrial permeability transition pore (PTP), a large, high-conductance, non-specific channel spanning both the mitochondrial inner and outer membranes [3,5–7], and selective release of cytochrome *c* that activates the caspases, proteolytic proteins responsible for apoptotic cell death [6]. Although the PTP is regulated by Ca^{2+} [5], the Ca^{2+}-binding component has not yet been identified. To control cytosolic or matrix-free Ca^{2+} concentration, mitochondria are endowed with five known routes for the influx and efflux of Ca^{2+} across the inner membrane [1,8]. However, uptake or release of Ca^{2+} by inner membrane transport systems necessarily involves Ca^{2+} crossing the mitochondrial outer membrane as well. The protein entity responsible for this permeability has been largely overlooked because of a consensus conception that the outer mitochondria membrane is freely permeable to Ca^{2+}. The most plausible candidate for Ca^{2+} transport across the mitochondrial outer membrane is the voltage-dependent anion channel (VDAC). VDAC, also known as mitochondrial porin, is a large channel which transports anions, cations, and various metabolites including substrates and nucleotides [9–12]. Previous evidence suggests that VDAC is also a component of the PTP [3,13–18]. The permeability of VDAC to bivalent cations has not been determined, except for a single report [19] on *Paramecium aurelia* VDAC being impermeable to Ca^{2+}. In this study, we demonstrate that VDAC is permeable to Ca^{2+}, possesses Ca^{2+} binding sites, and that Ruthenium Red (RuR), La^{3+} and ruthenium amine binuclear complex (Ru360) which inhibited VDAC activity also inhibited PTP opening in isolated mitochondria. We suggest that the Ca^{2+}-binding site(s) of VDAC is/are involved in the regulation of the outer membrane permeability and PTP, of which VDAC is a structural and functional component [3,13–18].

EXPERIMENTAL

Materials

Tris, Hepes, NaCl, PMSF, leupeptin, Triton X-100, Nonidet P-40, and Reactive Red-agarose were purchased from Sigma. Asolactin (soya bean phospholipids) was obtained from Associated Concentrates (Woodside, N.Y., U.S.A.). Alkaline phosphatase-conjugated goat anti-(mouse IgG) was purchased from Promega. VDAC-monoclonal antibody prepared against the N-terminal region of 31HL human porin (clone number 173/045; catalogue number 529538-B) and cyclosporin A were obtained from Calbiochem. Hydroxyapatite (Bio-Gel HTP) was purchased from Bio-Rad, Celite was obtained from BDH–Merck and RuR (97% pure) from Fluka.

Membrane and VDAC preparations

Liver mitochondria were isolated from rats as described previously [20], except that 0.1 mM PMSF and 0.5 μg/ml leupeptin

Abbreviations used: ANT, adenine nucleotide translocase; DCCD, dicyclohexylcarbodi-imide; OMM, outer mitochondrial membrane; PLB, planar lipid bilayer; PTP, permeability transition pore; RuR, Ruthenium Red; Ru360, Ruthenium amine binuclear complex; VDAC, voltage-dependent anion channel.

[1] To whom correspondence should be addressed (e-mail vardasb@bgumail.bgu.ac.il).

as protease inhibitors were added to the solutions. The specific activity of succinate–cytochrome *c* oxidoreductase activity [21] before and after osmotic shock was used to follow the intactness of the mitochondria. Succinate–cytochrome *c* oxidoreductase activity was zero before and 127.1 ± 0.5 nmol/mg ($n = 2$) after the osmotic shock. Thus the intactness of the mitochondria was over 99 %. VDAC was purified from rat liver mitochondria using hydroxyapatite and Reactive Red-agarose columns as described previously [22]. Using this method, the concentration of Triton X-100 was decreased from 3 to 0.4 %, and a concentrated and highly purified protein (over 98 %) was obtained. Protein concentration was determined according to Lowry et al. [23].

Ca^{2+}-uptake assay

Ca^{2+} uptake by freshly prepared rat liver mitochondria was assayed for 1–20 min at 30 °C in the presence of 220 mM mannitol, 70 mM sucrose, 0.5 mM nitrilotriacetic acid, 120 μM $CaCl_2$ (containing $^{45}Ca^{2+}$ at 3×10^4 c.p.m./nmol) (free $[Ca^{2+}] = 33.6$ μM), 15 mM Tris/HCl, pH 7.2, 0.5 mg/ml of mitochondria and 5 mM succinate and 0.1 mM P_i, or 3mM $MgCl_2$ and 4 mM ATP. Uptake was terminated by rapid Millipore filtration, followed by washing with 5 ml of 0.15 M KCl. Free Ca^{2+} concentration was calculated with a computer program WinMAXC 2.05 [24], using a Log stability constant for nitrilotriacetic acid and Ca^{2+} complex of 6.5. The maximal Ca^{2+} accumulated in the mitochondria was between 500–700 nmol/mg of protein (about 20 preparations). It should be noted that in the presence of succinate and P_i, Ca^{2+} accumulation is transient; it reached a maximal level, and then rapidly decreased to less than 1–2 % of its maximal value (reflecting PTP opening). The time course of this transient Ca^{2+} accumulation is affected by the Ca^{2+} and P_i concentrations. Accordingly, 120 μM Ca^{2+} and 0.1 mM P_i were chosen to generate a convenient time course. In the experiments in which the effects of different compounds on PTP opening, monitored by Ca^{2+} accumulation, were tested, the experiment was conducted as follows: first the time course of Ca^{2+} accumulation by the mitochondria was determined, from which the time of PTP opening was obtained. In the second experiment, the time course of Ca^{2+} accumulation was determined, and at the time in which it reached maximal level (determined in the first experiment), an aliquot was transferred to a tube containing Ru360, and the amount of Ca^{2+} accumulated in the control and Ru360 containing sample was followed as a function of time.

Mitochondrial swelling

Ca^{2+}-induced mitochondrial swelling was assayed under the same conditions as for Ca^{2+} accumulation, except that the temperature was 24 °C. Swelling was initiated by the addition of Ca^{2+} to the sample cuvette, and the absorbance changes at 520 nm were monitored every 15 s with a Genesys 5 spectrophotometer (Spectronics Instruments, Rochester, NY, U.S.A.).

VDAC activity

Reconstitution of purified VDAC into planar lipid bilayers (PLBs), single channel current recording and data analysis were carried out as described previously [22,25]. Briefly, PLB were prepared from soya bean asolactin dissolved in *n*-decane (50 mg/ml). Only PLBs with a resistance greater than 100 GΩ, were used. Purified VDAC (about 1 ng) was added to the *cis* chamber. After one or a few channels had inserted into the PLB, the excess protein was removed by washing the *cis* chamber with 20 volumes of solution to prevent further incorporation. Currents were recorded under voltage-clamp using a Bilayer Clamp (Warner Instruments, Hamden, CT, U.S.A.). The currents were measured with respect to the *trans* side of the membrane (ground). The currents were low-pass filtered at 1 kHz, using a Bessal filter (Frequency Devices, Haverhill, MA, U.S.A.) and digitized on-line using a Digidata 1200 interface board and pCLAMP 6 software (Axon Instruments). Sigma Plot 5.0 scientific software (Jandel Scientific) was used for curve fitting. In all experiments the bilayer was stable in the presence of La^{3+} or RuR, and both cations had no effect on the gramicidin-mediated current. The sonication–freeze–thaw method was used to prepare VDAC-containing and protein-free liposomes. The final concentration of Triton X-100 in all liposome preparations was 0.08 % (v/v). Three freeze–thaw cycles were performed during which liposomes were loaded with 5 mM $CaCl_2$ (containing $^{45}Ca^{2+}$ 200 c.p.m./nmol). Efflux of trapped Ca^{2+} was assayed by 25-fold dilution into a solution identical with that used in liposome preparation (0.15 M NaCl and 10 mM Tris, pH 7.4), and after 10 min the sample was filtered through Mixed Cellulose Ester filter (ME-30, 0.3 μm; Schleicher and Schuell, Keene, NH, U.S.A.), followed by two washes (4 ml each). Radioactivity was counted using a scintillation counter.

Other methods

SDS/PAGE was performed according to Laemmli [26] and Western-blot analysis was carried out according to standard procedure [27]. Succinate–cytochrome *c* oxidoreductase activity of the various mitochondrial preparations was assayed following cytochrome *c* reduction as described previously [21], except that ATP was omitted from the reaction mixture. The synthesis of Ru360 was carried out as described by Ying et al. [28].

RESULTS

VDAC reconstituted into a lipid bilayer is permeable to Ca^{2+}

Highly purified VDAC ([22] and Figure 1A) was reconstituted into PLB as a single channel and studied under voltage-clamp conditions in the presence of a $CaCl_2$ or NaCl concentration gradient. Examples of current records in response to a voltage

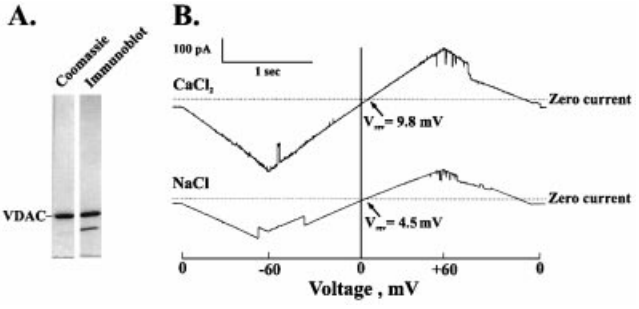

Figure 1 VDAC reconstituted into planar lipid bilayer is permeable to Ca^{2+}

(**A**) VDAC, purified as described in the Experimental section, is shown following SDS/PAGE and staining with Coomassie Blue (Coomassie) or electroblotting and immunostaining using a monoclonal anti-VDAC antibody (Immunoblot). (**B**) VDAC reconstitution into PLB was carried out as described previously [22,25]. Single-channel currents through VDAC in response to voltage ramps (−60–+60 mV at 62.5 mV/s) in the presence of a NaCl or $CaCl_2$ concentration gradient (150–500 mM) were recorded. The broken line indicates the zero current level and the arrows indicate the reversal potential V_{rev}. This is a representative experiment of a total of six experiments.

Table 1 Conductance and permeability of VDAC to $CaCl_2$

The zero-current potential (reversal potential, V_{rev}) and slope conductance (G_{slope}) were estimated from experiments similar to the one presented in Figure 1(B) carried out at the indicated NaCl or $CaCl_2$ concentration gradient. Relative permeability ($P_{Ca^{2+}}/P_{Cl^-}$) was estimated from equation 1 (see also Appendix, equation A9). The $CaCl_2$ activity coefficients (between 0.48–0.52) used in these calculations were as described previously [60], and were found to be similar to the ones we have determined experimentally by measuring the potential across an artificial cation-selective membrane (Ionac, 3470) separating solutions of the two different $CaCl_2$ concentrations. P_{Na^+}/P_{Cl^-} was calculated as in [22]. The results are the means ± S.E.M. of three independent experiments. The S.E.M. for P_{C^+}/P_{A^-} was calculated from three independent experiments.

	Conductance parameters		
Salt (mM) (*trans*:*cis*)	V_{rev} (mV)	G_{slope} (nS)	P_{C^+}/P_{A^-}
$CaCl_2$ (150:250)	4.85 ± 0.44	1.54 ± 0.12	0.35 ± 0.03
$CaCl_2$ (150:500)	9.85 ± 1.0	2.19 ± 0.06	0.37 ± 0.04
NaCl (150:500)	5.00 ± 0.2	1.40 ± 0.1	0.73 ± 0.03

ramp are shown (Figure 1B). Transitions between the main conductance and subconductance states of VDAC, the well-defined voltage-dependent characteristics of VDAC activity, are clearly seen in both $CaCl_2$ and NaCl solution.

To assess the Ca^{2+} permeability of VDAC (relative to chloride), the reversal potential was determined at different $CaCl_2$ concentration gradients. An increase in the $[Ca^{2+}]_{cis}$ shifted the reversal potential to more positive potentials (Table 1). An estimation of the Ca^{2+}/Cl^- permeability ratio was obtained using the reversal potential (V_{rev}), the $CaCl_2$ activity and the following equation (see the Appendix):

$$r = \frac{P_{Ca^{2+}}}{P_{Cl^-}} = \frac{(1+B)}{4}\left\{\frac{B[Cl^-]_0 - [Cl^-]_x}{[Ca^{2+}]_0 - [Ca^{2+}]_x B^2}\right\} \quad (1)$$

where $B = e^{\frac{F}{RT}V_{rev}}$.

Table 1 summarizes the results of VDAC conductance and permeability to Ca^{2+} in comparison with those for Cl^- and Na^+. The P_{Na^+}/P_{Cl^-} permeability ratio was estimated as described previously [22]. The estimated permeability ratios $P_{Ca^{2+}}/P_{Cl^-}$ and P_{Na^+}/P_{Cl^-} are 0.38 and 0.73, respectively, indicating that Ca^{2+} is only about 2.6 times and 1.3 times less permeable than Cl^- and Na^+, respectively (Table 1). Similar experiments with $MgCl_2$ indicate that Mg^{2+} can also permeate through the VDAC (results not shown).

VDAC reconstituted into liposomes is permeable to Ca^{2+}

The Ca^{2+} permeability of VDAC was also tested by reconstitution of purified VDAC into liposomes. VDAC-containing proteoliposomes, loaded with $^{45}Ca^{2+}$, released their Ca^{2+} content upon dilution into Ca^{2+}-free medium. Such release was not obtained with denatured VDAC-containing or VDAC-free liposomes (Figure 2A). VDAC-mediated Ca^{2+} efflux was inhibited by La^{3+} with an apparent IC_{50} of about 30 μM (Figure 2B). RuR at 2–10 μM also inhibited Ca^{2+} efflux from VDAC-containing liposomes (results not shown). Similar results were obtained when Ca^{2+} influx into VDAC-containing liposomes (preloaded with EGTA instead of $CaCl_2$) was measured (results not shown).

La^{3+} modification of VDAC activity

La^{3+} (lanthanides) have been shown to interact with various Ca^{2+}-binding proteins [29], including the mitochondrial Ca^{2+} uniporter [30]. The effect of La^{3+} on VDAC single channel activity reconstituted into PLB was studied under voltage-step

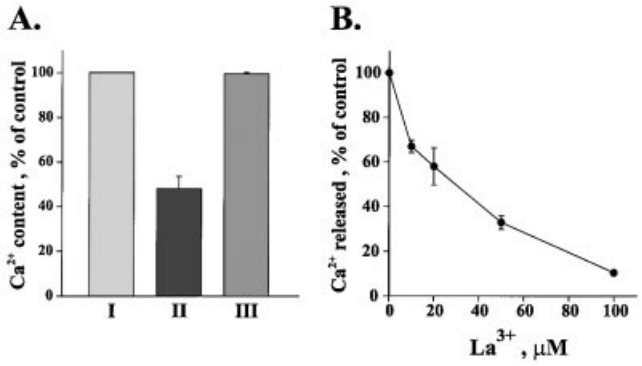

Figure 2 VDAC reconstituted into liposomes is permeable to Ca^{2+}

VDAC-containing and protein-free liposomes were prepared as described in the Experimental section. (**A**) VDAC-mediated Ca^{2+} efflux, where I, II and III indicate protein-free liposomes, VDAC-containing liposomes and heated VDAC-containing liposomes respectively. (**B**) La^{3+} inhibition of VDAC-mediated Ca^{2+} efflux. La^{3+} was added to loaded liposomes 1 min prior to their dilution. Ca^{2+} released from liposomes during 5 min (100%) was 19.2 and 8.3 nmol for (**A**) and (**B**) respectively. The results are averages from four separate experiments (each in duplicate).

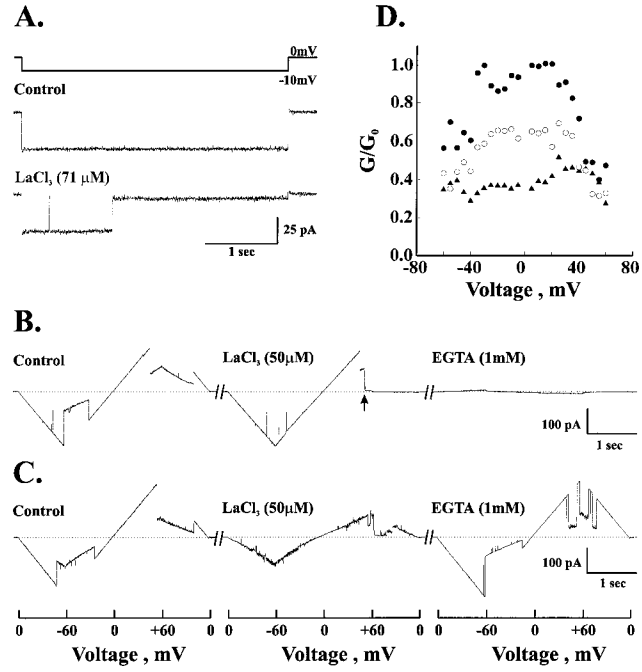

Figure 3 La^{3+} modification of VDAC activity

VDAC was reconstituted into PLB as in Figure 1(B) and single-channel or multichannel currents through VDAC were recorded. (**A**) Single channel current in response to voltage step before and after the addition of $LaCl_3$ is shown. In (**B**) and (**C**) representative recordings (in the presence of 1 M NaCl on both sides of the bilayer) of the effect of $LaCl_3$ on two different channels are shown. The re-opening by EGTA of the channel stabilized by La^{3+} at the sub-state ($n = 6$) (**C**), but not of the completely closed state ($n = 8$) (**B**). Multichannel (20 or more) recording (**D**) shows the relative conductance before (●) and after the addition of 100 μM $LaCl_3$ (▲) and subsequently of 1 mM EGTA (○). Relative conductance was determined by dividing the conductance (G) at a given voltage by the maximal conductance (G_0).

(Figure 3A) or voltage-ramp conditions (Figure 3B). La^{3+}, added to either side of the reconstituted VDAC, induced channel closure (Figure 3A). Single channel experiments, recorded at

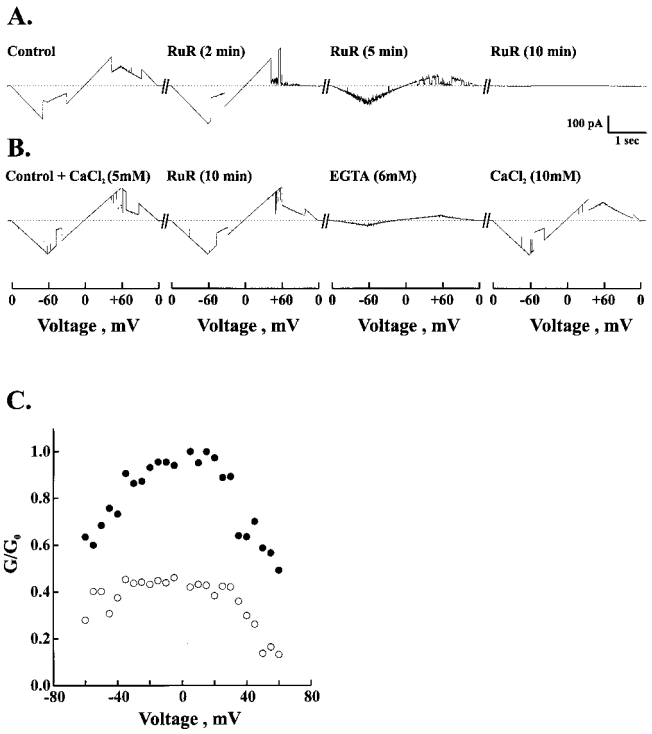

Figure 4 RuR inhibition of VDAC activity

VDAC, reconstituted into PLB as in Figure 1(B), was exposed to 50 μM RuR in the presence of 1 M NaCl (**A**) or 1 M NaCl and 5 mM $CaCl_2$ (**B**), and recordings were made at the indicated time or 2 min after the addition of the indicated compounds ($n = 7$). In (**C**) multichannel (about 10 channels) recordings of the average steady-state conductance of VDAC before (●) and 10 min after the addition of 5 μM RuR (○) as a function of voltage are shown.

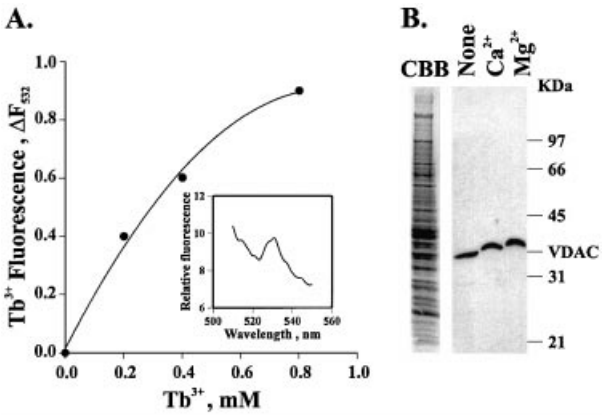

Figure 5 VDAC possesses a Ca^{2+}-binding site

(**A**) Tb^{3+} fluorescence was measured by excitation at 295 nm and recording the emission spectra of VDAC in the absence and the presence of the indicated concentration of Tb^{3+}. The background emission at 532 nm was subtracted from the measured emission at 532 nm to yield the change in Tb^{3+} fluorescence (ΔF_{532}). Inset shows representative emission spectrum of Tb^{3+} (0.4 mM) in the presence of VDAC (20 μg/ml). (**B**) Characteristic Ca^{2+}- and Mg^{2+}-induced shift in VDAC electrophoretic mobility. Brain synaptosomes [22] were incubated for 5 min with or without 5 mM of the indicated bivalent cation, and then subjected to SDS/PAGE followed by blotting and immunostaining using anti-VDAC antibody. CBB, Coomassie Brilliant Blue. Molecular-mass markers are shown on the right in kDa. Similar results were obtained with rat liver mitochondria and rabbit sarcoplasmic reticulum.

different voltages, demonstrated that La^{3+} inhibited the channel activity by stabilizing the channel in either a long-lived closed state with zero-conductance (Figure 3B), or in a sub-state with low conductance (Figure 3C). The inhibitory effect of La^{3+} was reversed by EGTA only when the channel was stabilized in the low-conducting state (Figure 3C), but not in the completely closed state (Figure 3B). In multichannel membrane, La^{3+} decreased channels conductance at all tested voltages and apparently eliminated the channel's voltage dependence (Figure 3D). The inhibition of multichannel activity by La^{3+} was only partially reversed by EGTA (Figure 3D). Tb^{3+}, as La^{3+}, also inhibited VDAC activity (results not shown).

RuR inhibition of VDAC activity

RuR is known as an inhibitor of the Ca^{2+} uniporter [30]. However, RuR was also reported to interact with several Ca^{2+}-binding proteins, including mitochondrial rapid mode system [31], Ca^{2+}-ATPase in the sarcoplasmic reticulum [32] and endoplasmic reticulum [33], Ca^{2+}-release channel/ryanodine receptor [34], calsequestrin [35] and calmodulin [36]. RuR was also shown to modify VDAC activity by lowering the voltage dependency of channel opening [37]. In the experiments presented here, RuR induced VDAC closure, in a time-dependent manner, stabilizing the channel in a completely closed state (Figure 4A). Ca^{2+}, in the presence of 1 M NaCl, prevented the inhibitory effect of RuR on VDAC activity. Chelation of Ca^{2+} with EGTA re-established RuR inhibition, and subsequent addition of $CaCl_2$ re-activated the channel (Figure 4B). Inhibition of VDAC activity by RuR is also observed in multichannel recording (Figure 4C). The inhibition by RuR was obtained at all tested voltages, however, the inhibition was more pronounced at positive voltages (Figure 4C). The results suggest that RuR interacts with Ca^{2+}-binding sites in the VDAC protein.

Table 2 RuR and La^{3+} inhibition of Ca^{2+} accumulation by isolated mitochondria

Rat liver mitochondria (0.5 mg/ml) were assayed for 1 min for ATP- or succinate-supported Ca^{2+} accumulation as described in the Experimental section, except for the assay of La^{3+} effect, nitrilotriacetic acid and P_i were omitted and the Ca^{2+} concentration was 33.6 μM. Control activities (100%) were 119.4 ± 3.4 ($n = 3$), 684 ± 15.8 ($n = 3$) and 140 ± 3.2 nmol/mg of protein per min for the Ca^{2+} accumulation assayed in the presence of ATP plus $MgCl_2$, succinate and P_i, and succinate respectively. RuR, Ru360 and La^{3+} were added to mitochondria 1 min before the $CaCl_2$ addition. The results are the mean ± S.D. of three experiments.

		Ca^{2+} accumulation (% of control)	
Additions	Energized with ...	ATP plus Mg^{2+}	Succinate
Control		100	100
RuR (0.1 μM)		24.9 ± 4.5	29.0 ± 3.8
RuR (0.5 μM)		5.6 ± 0.8	2.7 ± 0.2
Ru360 (0.1 μM)		8.4 ± 0.1	19.2 ± 0.5
Ru360 (0.5 μM)		3.1 ± 0.1	1.3 ± 0.1
La^{3+} (1 μM)		18.4 ± 1.4	16.2 ± 1.3
La^{3+} (5 μM)		6.1 ± 0.2	2.2 ± 0.1

VDAC possesses Ca^{2+}-binding sites

The following experiments directly demonstrated the presence of Ca^{2+}-binding site(s) in the VDAC molecule. Since Tb^{3+} inhibited VDAC activity, and the fluorescence from Tb^{3+} bound to a protein has been used as a sensitive probe of Ca^{2+}-binding sites in proteins [29], the interaction of Tb^{3+} with VDAC was tested.

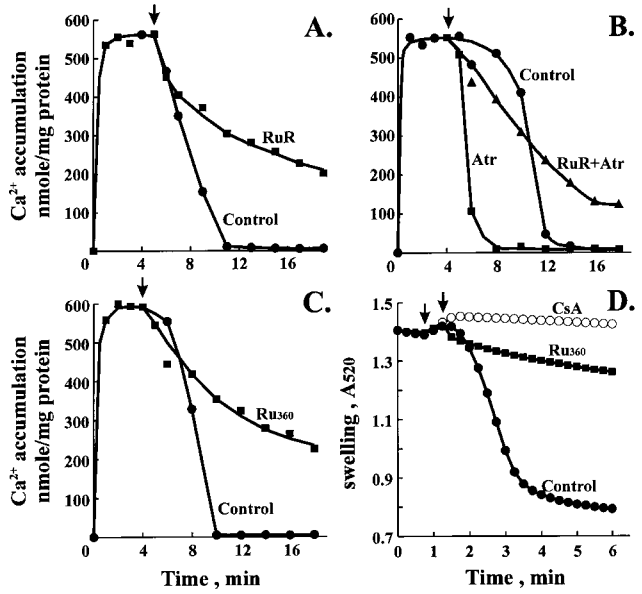

Figure 6 RuR and Ru360 inhibition of the permeability transition pore in mitochondria

Rat liver mitochondria (0.5 mg/ml) were assayed for succinate-supported Ca^{2+} accumulation and PTP opening as described in the Experimental section. (**A**) Ca^{2+} content of the mitochondria was assayed at the indicated time. RuR (1 μM) was added after Ca^{2+} accumulation reached a maximal level (indicated by the arrow). In (**B**) the experiment was carried out as described for (**A**), except that where indicated by an arrow, atractyloside (Atr; 5 μM) or RuR (5 μM) and atractyloside (5μM) were added. In (**C**) a similar experiment as in **A** was carried out, except that Ru360 (0.12 μM) was added at the indicated time (indicate by the arrow). In (**D**) the experiment was carried out as in (**C**), except that $^{45}Ca^{2+}$ was omitted, P_i was 0.1 mM and the swelling of mitochondria was followed by the decrease in A_{520} (as decribed in the Experimental section). The reaction was initiated by the addition of Ca^{2+} (120 μM; first arrow), and 30 s later cyclosporin A (CsA) (1 μM; second arrow) or Ru360 (0.12 μM; second arrow) were added. Each experiment in (**A**–**D**) is a representative of three different experiments.

Binding of Tb^{3+} to VDAC resulted in an enhanced green fluorescence (Figure 5A), suggesting that Tb^{3+} interacts with a specific site(s) on the VDAC molecule. As shown for different Ca^{2+}-binding proteins [38], a shift in the electrophoretic mobility was observed when $CaCl_2$ was added to purified VDAC or to mitochondria prior to electrophoresis, reflecting Ca^{2+} binding to VDAC. Mg^{2+} also induced a shift in VDAC mobility in SDS/PAGE (Figure 5B).

Inhibition by RuR, Ru360 and La^{3+} of Ca^{2+} accumulation in isolated rat liver mitochondria

Table 2 shows the inhibition by La^{3+}, RuR and Ru360 of succinate- or ATP-supported Ca^{2+} accumulation by freshly isolated rat liver mitochondria. Ru360 is a tervalent cation, shown to inhibit mitochondrial Ca^{2+} transport [28]. The inhibition of Ca^{2+} accumulation by La^{3+}, RuR and Ru360 was obtained at the same range of concentrations as reported previously for La^{3+} and RuR [30] and Ru360 [28].

PTP activation/opening is inhibited by RuR and Ru360

PTP opening in energized mitochondria was followed by monitoring Ca^{2+} content and large amplitude swelling (Figure 6). A transient Ca^{2+} accumulation in the mitochondria was observed; mitochondrial Ca^{2+} content was increased up to 500–700 nmol/mg of protein, and then rapidly decreased to 1–5 nmol/mg of protein (Figures 6A–6C). This transient Ca^{2+} retention suggests

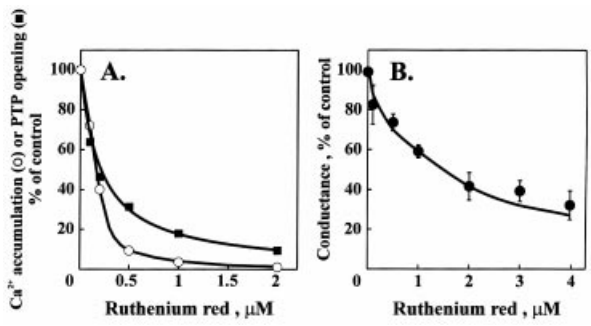

Figure 7 Concentration-dependence of RuR inhibition of Ca^{2+} accumulation and PTP opening in isolated mitochondria and of VDAC activity

(**A**) Ca^{2+} accumulation and PTP opening were assayed as described in Figure 6, with the following modifications: for Ca^{2+}-accumulation assay, RuR was added to mitochondria at zero time (without pre-incubation) and Ca^{2+} content was determined after 1 min; for monitoring PTP opening, RuR was added after maximal Ca^{2+} accumulation (5 min), and the Ca^{2+} content of the mitochondria was assayed 3 min after its addition. (**B**) VDAC activity was assayed as in Figure 4(C) for multichannel recordings. Recording was carried out 10 min after the addition of the indicated concentration RuR. The results were fitted with the following equation:

$$A/A_{max} = [RuR]^h/([RuR]^h + IC_{50}^h)$$

where A is the activity of Ca^{2+} accumulation, PTP opening or VDAC conductance (assuming maximal inhibition of 80%), at a given concentration of RuR ([RuR]), A_{max} is the maximum activity (in the absence of RuR), IC_{50} is the concentration of RuR that decreases the activity by 50%. The best fit was obtained with Hill coefficient (h) of 1.

that the mitochondria have undergone the permeability transition, losing the accumulated Ca^{2+} via the PTP [5,6,13,39–41]. The release of Ca^{2+} was prevented by RuR, when added after Ca^{2+} accumulation had reached a maximal level, and before PTP is activated (Figure 6A). To evaluate the significance of the uniporter activity during PTP opening, unidirectional Ca^{2+} transport was followed by the addition of radiolabelled calcium ($^{45}Ca^{2+}$) to mitochondria preloaded with non-labelled calcium ($^{40}Ca^{2+}$) after PTP activation. No significant $^{45}Ca^{2+}$ influx was evident either in the absence or the presence of RuR (results not shown). The result of this experiment suggest that the effect of RuR on PTP opening is not mediated by inhibition of the uniporter, while supporting the suggestion of the VDAC involvement in PTP.

Since La^{3+} precipitated as a complex with P_i or acetate (even at low concentrations), its effect of on PTP opening was not determined. The adenine nucleotide translocase (ANT) inhibitors carboxyatractyloside [42] and atractyloside [43] were shown to activate PTP opening. Figure 6(B) shows that atractyloside promoted onset of the PTP, whereas RuR opposed the onset. To our knowledge, an interaction of RuR with the ANT has not been reported. Therefore, RuR effect on PTP opening may be mediated by its interaction with VDAC.

Mitochondrial swelling was obtained approx. 1 min after Ca^{2+} addition to energized mitochondria, and this swelling was prevented by cyclosporin A (1 μM) (Figure 6D). Demonstration of the effect of RuR on mitochondrial swelling is technically difficult because of its absorbance spectrum. Thus Ru360, which has a maximal absorbance at 360 nm and no absorbance at 520 nm, was used. Ru360, at relatively low concentrations, inhibited the Ca^{2+}-induced PTP opening/assembly as followed by monitoring the transient Ca^{2+} accumulation (Figure 6C). Ru360 inhibited the subsequent mitochondrial large amplitude swelling, as assessed by the change in light scattering (Figure 6D). Ru360 also inhibited the channel activity of purified VDAC reconstituted into PLB (results not shown).

Correlation between RuR inhibition of Ca^{2+} accumulation, PTP opening and VDAC activity

The concentration-dependence of RuR inhibition on Ca^{2+} accumulation and PTP opening in mitochondria, and of VDAC activity reconstituted into PLB, are shown in Figure 7. Ca^{2+} accumulation and PTP opening were inhibited by RuR with an IC_{50} of approx. 0.25 μM and 0.3 μM, respectively, and 90–100 % inhibition at 1–2 μM RuR. The average conductance of VDAC activity reconstituted into PLB was inhibited by RuR with IC_{50} of 1.0 μM and was 80 % inhibited at approx. 4 μM RuR. The concentration of RuR that yielded 50 % inhibition of VDAC activity is low relative to the concentrations that produced inhibition of other Ca^{2+}-binding proteins, such as the Ca^{2+}-ATPase in the sarcoplasmic reticulum [32] and the Ca^{2+}-release channel/ryanodine receptor [34]. The difference in sensitivity of VDAC activity and of the mitochondrial Ca^{2+} accumulation and PTP opening may result from the fact that VDAC was solubilized with, and deeply buried, in Triton X-100 [44]. It has been shown that a trace amount of Triton X-100 modifies the sensitivity of the mitochondrial VDAC to the polyanion inhibitor [45].

DISCUSSION

The outer mitochondrial membrane (OMM), as the boundary structure of the mitochondria, plays a central role in mediating complex interactions between mitochondria metabolic and genetic systems and the other parts of the cell [46,47]. Generally, the OMM has not been considered as a barrier to transport, due to the presence of VDAC, which was assumed to be freely permeable to ions and uncharged molecules. Recently, however, this view has been changed, as demonstrated by recent findings that OMM permeability is regulated via VDAC, and thereby VDAC can control coupled respiration and cell survival [48]. The results presented here support this concept, and further suggest the involvement of VDAC in the regulation of cytosolic and mitochondrial Ca^{2+} concentration, and in PTP assembly and/or activation.

VDAC Ca^{2+} permeability

The results indicate that VDAC is highly permeable to Ca^{2+}, as it is only about 2.6 times and 1.3 times less permeable than Cl^- and Na^+ respectively (Table 1). Thus VDAC as an OMM protein provides the pathway for Ca^{2+} transport into and out of the mitochondria. The discrepancy between the results presented here and the previous report by Schein et al. [19] that VDAC from *Paramecium* is impermeable to Ca^{2+} may reflect differences between VDAC from mammalian and *Paramecium*. The results presented here suggest the involvement of VDAC in Ca^{2+} transport in mitochondria, thereby, in Ca^{2+} homoeostasis.

VDAC Ca^{2+}-binding sites

The primary amino acid sequence of VDAC1, as deduced from cDNA sequence, contains no features of an EF-hand structure which is a high-affinity Ca^{2+}-binding site. However, an aspartate-rich region (within residues 126–130), located within the transmembrane domain, is a potential low-affinity Ca^{2+}-binding site. Several lines of evidence suggest that VDAC possesses Ca^{2+}-binding site(s) (Figures 3–5). These include: Tb^{3+}-enhanced fluorescence in the presence of VDAC (Figure 5A); Ca^{2+}-induced shift in VDAC electrophoretic mobility (Figure 5B); RuR inhibition of VDAC activity and its reversal by Ca^{2+} (Figure 4); inhibition of VDAC activity by La^{3+} (Figure 3). The nature of one or more of the bivalent binding site(s) may be reflected in the inability of EGTA to re-open some channels that were completely closed by La^{3+}. This may suggest that La^{3+} interacts with a site located within the pore in which it became occluded, thereby, not exposed to EGTA.

Dicyclohexylcarbodi-imide (DCCD) that reacts specifically with carboxyl groups, has been shown to specifically label VDAC [25,49,50] and to inhibit VDAC activity [25,50]. Since DCCD modifies Ca^{2+}-binding sites [49], it is possible that DCCD modifies VDAC activity by binding to a carboxyl group located at a Ca^{2+}-binding site(s). De Pinto et al. [49] identified Glu^{72} as the DCCD-binding amino acid in VDAC from bovine heart mitochondria. The presence of two metal-binding sites on VDAC has been suggested, based on the effect of aluminium on the voltage-dependence of VDAC [51].

A regulatory function of Ca^{2+} could not be demonstrated in channel activity of purified VDAC reconstituted into PLB. This may result from Triton X-100 modification of Ca^{2+} binding or the effect of Ca^{2+} on VDAC activity. Trace amounts of Triton X-100 were found to modify the sensitivity of the mitochondrial VDAC to the polyanion inhibition [45]. The effects of La^{3+} and RuR on VDAC activity may be due to their higher affinity for Ca^{2+}-binding sites. However, as shown for a variety of Ca^{2+}-binding proteins [29,35], it is also possible that binding of La^{3+} or RuR, but not of Ca^{2+}, to VDAC cation binding sites induced channel closure (Figures 3 and 4), and such inhibition can be observed more easily than stimulation of highly active channels. The activation of PTP opening by Ca^{2+} and its inhibition by RuR and Ru360 (Figure 6) are in line with such differential effects of Ca^{2+} and RuR or Ru360 on VDAC activity.

Interaction of RuR and La^{3+} with VDAC and inhibition of Ca^{2+} accumulation in mitochondria

RuR and La^{3+} had been reported previously to inhibit mitochondrial Ca^{2+} uptake, and the mitochondrial uniporter was suggested as their target [30,31]. However, direct interaction of RuR or La^{3+} with the uniporter was not demonstrated. The Ca^{2+} uniporter has been studied for over 25 years, yet its molecular identity is unknown. An 18 kDa protein has been suggested as the mitochondrial Ca^{2+} uniporter, and its Ca^{2+}-transport activity displayed a very low sensitivity to RuR [52]. If the positively charged RuR (hexavalent) and La^{3+} inhibit Ca^{2+} uptake in mitochondria by interaction with the uniporter, located at the inner mitochondrial membrane, their penetration of the outer mitochondrial membrane is required. As polycations, the permeability of RuR and La^{3+} through the membrane must be very low. Since La^{3+} and RuR inhibited VDAC activity, we suggest that their inhibitory effect on mitochondrial Ca^{2+} accumulation may result from interaction and inhibition of VDAC permeability to Ca^{2+}. This, however, does not rule out a possible direct interaction of RuR and La^{3+} with intramitochondrial targets.

Involvement of VDAC in the activity and regulation of PTP

The mitochondrial PTP is induced by a variety of apoptotic inducers such as elevated levels of Ca^{2+} in the matrix. The role of mitochondria in apoptosis also emerged from demonstrations of interactions between PTP component(s) and regulatory proteins of apoptosis (e.g. Bcl-2, Bax) [3,53,54].

When respiring mitochondria take up Ca^{2+}, in the absence of nucleotides, the accumulated Ca^{2+} is subsequently released via a Ca^{2+}-dependent pore, referred to as the PTP. The mitochondrial target for PTP activating Ca^{2+} has not been precisely defined. While Ca^{2+} induce opening of PTP, other metal ions (Me^{2+}) generally behave as pore inhibitors [5,55,56]. Two separate Me^{2+} binding sites on PTP regulate its activity. While Ca^{2+}, and other

Me^{2+} binding to external site decreases pore opening, the occupancy of an internal site by Ca^{2+} increases pore opening [55,56]. Binding of other Me^{2+} to this site inhibits pore opening and apparently competes with Ca^{2+} [5,55,56]. Thus, Ca^{2+} affect the PTP open–closed transitions by binding to an external or internal site, causing a decrease or an increase in the open probability of the pore, respectively. Despite the attention that Ca^{2+} has been given as a modulator of PTP, its specific site of interaction in the PTP complex remains unknown. In addition to the ANT and cyclophilin D in the inner mitochondrial membrane, it is well established that VDAC, at the outer membrane, is a major component of the PTP [3,13–18,54]. In isolated mitochondria, the Ca^{2+} release observed after matrix Ca^{2+} concentration reaches a maximal level, reflecting PTP opening, was inhibited by RuR and Ru360 (Figures 6 and 7). The inhibitory effect of RuR and Ru360 on PTP opening/assembly is not due to their interaction with the Ca^{2+} uniporter, since they were added after that Ca^{2+} uptake reached a maximal level, and inhibition of the uniporter should increase and not decrease Ca^{2+} efflux. Thus a possible involvement of the Ca^{2+}-binding sites of VDAC in the modulation of PTP activity is suggested, and that La^{3+}, RuR and Ru360 may have interacted with these sites. Atractylate induces the PTP through an undefined mechanism that may involve conformational changes of ANT [42,43]. RuR inhibited PTP opening activated by atractyloside (Figure 6). To our knowledge, direct interaction of RuR or Ca^{2+} with ANT has not been reported, although modulation of the ANT by Ca^{2+} has been suggested [41,57], thus RuR inhibition of PTP activation may result from interaction with a protein distinct from ANT. Since VDAC is a component of PTP [3,13–18,54] and possesses Ca^{2+}-binding sites (Figures 3–5) that bind RuR (Figure 4), we suggest that the Ca^{2+}-binding sites of VDAC are involved in the regulation of PTP activity. One possible mechanism of RuR inhibition of PTP opening involves inhibition of VDAC conductance, thereby, of PTP permeability (as with VDAC in PLB; Figure 4). Binding of Ca^{2+} to VDAC may thus result in pore opening, while occupation of these sites by RuR led to pore closure (see above).

The results support the accumulating evidence for VDAC being a component of PTP [3,13–18,54], and further suggest that VDAC plays a regulatory role in PTP opening and/or assembly. The reported inhibitory effects of RuR and La^{3+} on apoptosis and necrosis [58] may be due to impairment of Ca^{2+} transport through VDAC or modulating its activity via interaction with the Ca^{2+}-binding sites.

Involvement of VDAC in intracellular Ca^{2+} signalling

It is now accepted that there is interplay between mitochondrial function and cellular Ca^{2+} signalling [47,59]. Extensive evidence indicates that changes in intramitochondrial Ca^{2+} concentration are followed by dysfunction of mitochondrial metabolism, leading to apoptosis, carcinogenesis, and cell injury associated with ischaemia [3,18,41]. VDAC, as the outer mitochondrial membrane protein, providing the pathway for Ca^{2+} transport into and out of mitochondria, must thereby have a role in intracellular Ca^{2+} signalling.

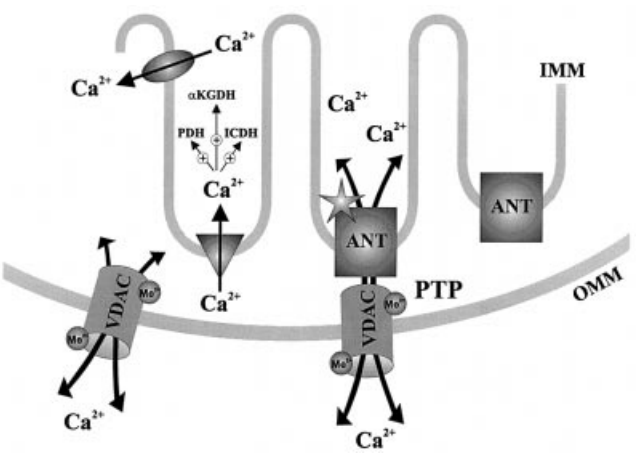

Figure 8 The role of VDAC in mitochondrial Ca^{2+} transport and in the regulation of mitochondrial functions

Ca^{2+}-influx and -efflux transport systems in the inner mitochondrial membrane (IMM) are shown as triangle and oval symbols respectively. The activation by intramitochondrial Ca^{2+} of pyruvate dehydrogenase (PDH), isocitrate dehydrogenase (ICDH) and α-ketoglutarate dehydrogenase (αKGDH) is shown. VDAC in the OMM is presented as a Ca^{2+} channel possessing internal and external metal binding sites (Me^{2+}). VDAC as a constituent of the PTP is represented as the Ca^{2+}-transport pathway and as the Me^{2+}-sensitive target. The ANT and cyclophilin D (star shape) are shown as components of the PTP.

A model for the role of VDAC in Ca^{2+} transport and regulation of mitochondrial functions is summarized in Figure 8. The model suggests that VDAC is responsible for the OMM Ca^{2+} permeability, and that its capability to bind metals (Me^{2+}) has an important function in cellular and mitochondrial Ca^{2+} homoeostasis. The coupling between the increase in cytosolic and mitochondrial Ca^{2+} is a possible mechanism that coordinates mitochondrial ATP production upon cellular energy demand. VDAC, as a protein transporting both ATP and Ca^{2+}, and possessing regulatory binding site(s) for Me^{2+}/Ca^{2+}, most likely play a crucial role in this coordination. PTP, which act as the Ca^{2+} release channel, contributes to the development of pathological processes [39,56]. Thus VDAC may mediate Ca^{2+} regulation of PTP by providing the pathway for Ca^{2+} influx and efflux, into and from the mitochondria, and the regulatory binding Me^{2+}/Ca^{2+} sites.

The work was supported by grants from the Israeli Science Foundation. We thank Dr Martin Pring (Department of Physiology, University of Pennsylvania, Pennsylvania, U.S.A.) for developing the equation for calculating Ca^{2+} permeability. We thank Dr C. Aflalo for reading the manuscript and providing valuable suggestions and Mr A. Israelson for the synthesis of Ru360.

APPENDIX

The Nernst–Planck equation describing the flux ϕ_i of an ionic species i across a diffusion path $x(0_i \leqslant x \leqslant X)$, subjected to a chemical gradient $d[I]/dx$ and an electrical gradient dV/dx can be written as follows:

$$\phi_i = D_i \frac{d[I]x}{dx} + D_i \frac{F}{RT} \cdot \frac{dV}{dx} z_i [I]x \qquad \text{(A1)}$$

Assuming the same diffusion constant D_i for both terms and that the electrical gradient across the membrane considered as a constant, one can rearrange equation (A1) as:

$$\frac{\phi_i}{D_i} = \frac{d[I]x}{dx} + \beta[I]x \quad \text{where } \beta = \frac{F}{RT} \cdot \frac{dV}{dx} z_i = \text{constant} \qquad \text{(A2)}$$

Assuming that at steady state the flux is independent of x, the position in the diffusing path, one can integrate the non-

homogeneous differential equation of the first order, equation (A2), using the boundary condition $[I]_{x=0} = [I]_0 = \text{constant}$, to produce:

$$[I]x = \frac{\phi_i}{D_i\beta} + \left\{ [I]_0 - \frac{\phi_i}{D_i\beta} \right\} e^{-\beta x} \tag{A3}$$

Or in terms of the flux:

$$\phi_i = \frac{D_i\beta\{[I]_0 - [I]_x e^{\beta x}\}}{1 - e^{\beta x}} \tag{A4}$$

At the secondary boundary $x = X$, and $[I]_x = [I]_X$, the product $(dV/dx)X$ represents, in fact, the measured voltage V_m, so that equation (A4) becomes:

$$\phi_i = \frac{D_i \frac{F}{RT} z_i \frac{dV}{dx} \{[I]_0 - [I]_x e^{\frac{F}{RT} z_i V_m}\}}{1 - e^{\frac{F}{RT} z_i V_m}} \tag{A5}$$

We recall that at the reversal potential V_{rev} (Figure 1):

$$I_{rev} = F \sum_i z_i \phi_i = 0 \tag{A6}$$

Denoting the permeability $P_i = D_i/X$ and $B = e^{(F/RT)V_m}$, one can combine equations (A5) and (A6) to obtain:

$$\sum_i z_i^2 P_i \frac{\{[I]_0 - [I]_x B^{z_i}\}}{1 - B^{z_i}} = 0 \tag{A7}$$

Which reduces to the Goldman–Hodgkin–Katz equation for $z_i = \pm 1$.

In the case of $CaCl_2 \rightarrow Ca^{2+} + 2Cl^-$, equation (A7) yields:

$$4P_{Ca^{2+}} \frac{\{[Ca^{2+}]_0 - [Ca^{2+}]_x B^2\}}{1 - B^2} + P_{Cl^-} \frac{\{[Cl^-]_0 - [Cl^-]_x B^{-1}\}}{1 - B^{-1}} = 0 \tag{A8}$$

And, therefore, the ratio of permeability coefficients of ions is given by:

$$r = \frac{P_{Ca^{2+}}}{P_{Cl^-}} = \frac{(1+B)}{4} \left\{ \frac{B[Cl^-]_0 - [Cl^-]_x}{[Ca^{2+}]_0 - [Ca^{2+}]_x B^2} \right\}. \tag{A9}$$

REFERENCES

1 Gunter, T. E., Gunter, K. K., Sheu, S. S. and Gavin, C. E. (1994) Mitochondrial calcium transport: physiological and pathological relevance. Am. J. Physiol. **267**, C313–339

2 Di-Lisa, F., Gambassi, G., Spurgeon, H. and Hansford, R. G. (1993) Intramitochondrial free calcium in cardiac myocytes in relation to dehydrogenase activation. Cardiovasc. Res. **2**, 1840–1844

3 Crompton, M. (1999) The mitochondrial permeability transition pore and its role in cell death. Biochem. J. **341**, 233–249

4 McConkey, D. A. and Orrenius, S. (1997) The role of calcium in the regulation of apoptosis. Biochem. Biophys. Res. Commun. **239**, 357–366

5 Zoratti, M. and Szabo, I. (1995) The mitochondrial permeability transition. Biochim. Biophys. Acta **1241**, 139–176

6 Ichas, F. and Mazat, J.-P. (1998) From calcium signalling to cell death: two conformations for the mitochondrial permeability transition pore. Switching from low- to high-conductance state. Biochim. Biophys. Acta **1366**, 33–50

7 Liu, X., Kim, C. N., Yang, R., Jemmerson, R. and Wang, X. (1996) Induction of apoptotic program in cell–free extracts: requirement for dATP and cytochrome c. Cell **86**, 147–157

8 Gunter, T. E., Buntinas, L., Sparagna, G. C. and Gunter, K. K. (1998) The Ca^{2+} transport mechanisms of mitochondria and Ca^{2+} uptake from physiological-type Ca^{2+} transients. Biochim. Biophys. Acta **1366**, 5–15

9 Benz, R. (1994) Permeation of hydrophilic solutes through mitochondrial outer membranes: review on mitochondrial porins. Biochim. Biophys. Acta **1197**, 167–196

10 Mannella, C. A. (1997) Minireview: on the structure and gating mechanism of the mitochondrial channel, VDAC. J. Bioenerg. Biomembr. **29**, 525–531

11 Colombini, M. (1994) Anion channel in the mitochondrial outer membrane. Curr. Top. Membr. Transp. **42**, 73–101

12 Hodge, T. and Colombini, M. (1997) Regulation of metabolite flux through voltage-gating of VDAC channels. J. Membr. Biol. **157**, 271–279

13 Szabo, I. and Zoratti, M. (1993) The mitochondrial permeability transition pore may comprise VDAC molecules. I. Binary structure and voltage dependence of the pore. FEBS Lett. **330**, 201–205

13a Szabo, I., De Pinto, V. and Zoratti, M. (1993) The mitochondrial permeability transition pore may compromise VDAC molecules. II. The electrophysical properties of VDAC are compatible with those of the mitochondrial megachannel. FEBS Lett. **330**, 206–210

14 Beutner, G., Ruck, A., Riede, B., Welte, W. and Brdiczka, D. (1996) Complexes between kinases, mitochondrial porin and adenylate translocator in rat brain resemble the permeability transition pore. FEBS Lett. **396**, 189–195

15 Shimizu, S., Narita, M. and Tsujimoto, Y (1999) Bcl-2 family proteins regulate the release of apoptogenic cytochrome *c* by the mitochondrial channel VDAC. Nature (London) **399**, 483–487

16 Shimizu, S., Konishi, A., Kodama, T. and Tsujimoto, Y. (2000) BH4 domain of anti-apoptotic Bcl-2 family members closes voltage-dependent anion channel and inhibits apoptotic mitochondrial changes and cell death. Proc. Natl. Acad. Sci. U.S.A. **97**, 3100–3105

17 Shimizu, S., Ide, T., Yanagida, T. and Tsujimoto, Y. (2000) Electrophysiological study of a novel large pore formed by Bax and the voltage-dependent anion channel that is permeable to cytochrome *c*. J. Biol. Chem. **275**, 12321–12325

18 Perez Velazauez, J. L., Frantseva, M. V., Huzar, D. V. and Carlen, P. L. (2000) Mitochondrial porin required for ischemia-induced mitochondrial dysfunction and neuronal damage. Neuroscience **97**, 363–369

19 Schein, S. J., Colombini, M. and Finkelstein, A. (1976) Reconstitution in planar lipid bilayers of a voltage-dependent anion-selective channel obtained from *Paramecium* mitochondria. J. Membr. Biol. **30**, 99–120

20 Johnson, D. and Lardy, H. (1967) Isolation of liver or kidney mitochondria. Methods Enzymol. **10**, 94–96

21 Mannella, C. A. (1987) Mitochondrial outer membrane channel (VDAC, porin) two-dimensional crystals from *Neurospora*. Methods Enzymol. **148**, 453–465

22 Gincel, D., Silberberg, S. D. and Shoshan-Barmatz, V. (2000) Modulation of the voltage-dependent anion channel (VDAC) by glutamate. J. Bioenerg. Biomembr. **32**, 571–583

23 Lowry, O. H., Rosebrough, N. J., Farr, A. L. and Randall, R. J. (1951) Protein measurements with Folin phenol reagent. J. Biol. Chem **193**, 265–275

24 Bers, D. M., Patton, C. W. and Nuccitelli, R. A. (1994) Practical guide to the preparation of Ca^{2+} buffers. Methods Cell Biol. **40**, 3–29

25 Shoshan-Barmatz, V., Hadad, N., Feng, W., Shafir, I., Orr, I., Varsanyi, M. and Heilmeyer, L. M. (1996) VDAC/porin is present in sarcoplasmic reticulum from skeletal muscle. FEBS Lett. **386**, 205–210

26 Laemmli, U. K. (1970) Cleavage of structural proteins during the assembly of the head of bacteriophage T4. Nature (London) **227**, 680–685

27 Towbin, H., Staehelin, T. and Gordon, J. (1979) Electrophoretic transfer of proteins from polyacrylamide gels to nitrocellulose sheets: procedure and some applications. Proc. Natl. Acad. Sci. U.S.A. **76**, 4350–4354

28 Ying, W. L., Emerson, J., Clarke, M. J. and Sanadi, D. R. (1991) Inhibition of mitochondrial calcium ion transport by an oxo-bridged dinuclear ruthenium amine complex. Biochemistry **30**, 4949–4952

29 Hadad, N., Abramson, J. J., Zable, T. and Shoshan-Barmatz, V. (1994) Ca^{2+} binding sites of the ryanodine receptor/Ca^{2+} release channel of sarcoplasmic reticulum. Low affinity binding site(s) as probed by terbium fluorescence. J. Biol. Chem. **269**, 24864–24869

30 Reed, K. C. and Bygrave, F. L. (1974) The inhibition of mitochondrial calcium transport by lanthanides and ruthenium red. Biochem. J. **140**, 143–155

31 Sparagna, G. C., Gunter, K. K., Sheu, S. S. and Gunter, T. E. (1995) Mitochondrial calcium uptake from physiological-type pulses of calcium. A description of the rapid uptake mode. J. Biol. Chem. **270**, 27510–27515

32 Corbalan-Garcia, S., Teruel, J. A. and Gomez-Fernandez, J. C. (1992) Characterization of Ruthenium red-binding sites of the Ca^{2+}-ATPase from sarcoplasmic reticulum and their interaction with Ca^{2+}-binding sites. Biochem. J. **287**, 767–774

33 Meszaros, L. G. and Volpe, P. (1991) Caffeine- and ryanodine-sensitive Ca^{2+} stores of canine cerebrum and cerebellum neurons. Am. J. Physiol. **261**, C1048–C1054

34 Chen, S. R. and MacLennan, D. H. (1994) Identification of calmodulin-, Ca^{2+}-, and Ruthenium red-binding domains in the Ca^{2+} release channel (ryanodine receptor) of rabbit skeletal muscle sarcoplasmic reticulum. J. Biol. Chem. **269**, 22698–22704

35 Charuk, J. H., Pirraglia, C. A. and Reithmeier, R. A. (1990) Interaction of ruthenium red with Ca^{2+}-binding proteins. Anal. Biochem. **188**, 123–131

36 Sasaki, T., Naka, M., Nakamura, F. and Tanaka, T. (1992) Ruthenium red inhibits the binding of calcium to calmodulin required for enzyme activation. J. Biol. Chem. **267**, 21518–21523

37 Siadat, S., Reymann, S., Horn, A. and Thinnes, F. P. (1998) Studies on human porin XVIII: the multicompartment effector ruthenium red reduces the voltage dependence of human VDAC in planar lipid bilayers. Mol. Genet. Metab. **65**, 246–249

38 Gregersen, H. J., Heizmann, C. W., Kaegi, U. and Celio, M. R. (1990) Ca^{2+}-dependent mobility shift of parvalbumin in one- and two-dimensional gel electrophoresis. Adv. Exp. Med. Biol. **269**, 89–91

39 Lemasters, J. J., Qian, T., Bradham, C. A., Brenner, D. A., Cascio, W. E., Trost, L. C., Nishimura, Y., Nieminen, A. L. and Herman, B. (1999) Mitochondrial dysfunction in the pathogenesis of necrotic and apoptotic cell death. J. Bioenerg. Biomembr. **31**, 305–319

40 Haworth, R. A. and Hunter, D. R. (1980) Allosteric inhibition of the Ca^{2+}-activated hydrophilic channel of the mitochondrial inner membrane by nucleotides. J. Membr. Biol. **54**, 231–236

41 Halestrap, A. P. (1999) The mitochondrial permeability transition: its molecular mechanism and role in reperfusion injury. Biochem. Soc. Symp. **66**, 181–203

42 Novgorodov, S. A., Gudz, T. I., Brierley, G. P. and Pfeiffer, D. R. (1994) Magnesium ion modulates the sensitivity of the mitochondrial permeability transition pore to cyclosporin A and ADP. Arch. Biochem. Biophys. **311**, 219–228

43 Halestrap, A. P. (1987) The regulation of the oxidation of fatty acids and other substrates in rat heart mitochondria by changes in the matrix volume induced by osmotic strength, valinomycin and Ca^{2+}. Biochem. J. **244**, 159–164

44 De Pinto, V., Benz, R. and Palmieri, F. (1989) Interaction of non-classical detergents with the mitochondrial porin. A new purification procedure and characterization of the pore-forming unit. Eur. J. Biochem. **183**, 179–187

45 Bathori, G., Fonyo, A. and Ligeti, E. (1995) Trace amounts of Triton X-100 modify the inhibitor sensitivity of the mitochondrial porin. Biochim. Biophys. Acta. **1234**, 249–254

46 Poyton, R. O. and McEwen, J. E. (1996) Crosstalk between nuclear and mitochondrial genomes. Ann. Rev. Biochem. **65**, 563–607

47 Rizzuto, R., Brini, M., Murgia, M. and Pozzan, T. (1993) Microdomains with high Ca^{2+} close to IP_3-sensitive channels that are sensed by neighboring mitochondria. Science (Washington, D.C.) **262**, 744–747

48 Vander-Heiden, M. G., Chandel, N. S., Li, Z. X., Schumacker, P. T., Colombini, M. and Thompson, C. B. (2000) Outer mitochondrial membrane permeability can regulate coupled respiration and cell survival. Proc. Natl. Scad. Sci. U.S.A. **97**, 4666–4671

49 De Pinto, V., Aljamal, J. A. and Palmier, F. (1993) Location of the dicyclohexylcarbodiimide-reactive glutamate residue in the bovine heart mitochondrial porin. J. Biol. Chem. **268**, 12977–12982

50 Shafir, I., Feng, W. and Shoshan-Barmatz, V. (1998) Dicyclohexylcarbodiimide interaction with the voltage-dependent anion channel from sarcoplasmic reticulum. Eur. J. Biochem. **253**, 627–636

51 Zhang, D. W. and Colombini, M. (1990) Group IIIA-metal hydroxides indirectly neutralize the voltage sensor of the voltage-dependent mitochondrial channel, VDAC, by interacting with a dynamic binding site. Biochim. Biophys. Acta **1025**, 127–134

52 Zazueta, C., Zafra, G., Vera, G., Sanchez, C. and Chavez, E. (1998) Advances in the purification of the mitochondrial Ca^{2+} uniporter using the labelled inhibitor ^{103}Ru360. J. Bioenerg. Biomembr. **30**, 489–498

53 Petit, P. X., Susin, S. A., Zamzami, N., Mignotte, B. and Kroemer, G. (1996) Mitochondria and programmed cell death: back to the future. FEBS Lett. **396**, 7–13

54 Marzo, I., Brenner, C., Zamzami, N., Susin, S. A., Beutner, G., Brdiczka, D., Remy, R., Xie, Z. H., Reed, J. C. and Kroemer, G. (1998) The permeability transition pore complex: a target for apoptosis regulation by caspases and bcl-2-related proteins. J. Exp. Med. **187**, 1261–1271

55 Bernardi, P., Veronese, P. and Petronilli, V. (1993) Modulation of the mitochondrial cyclosporin A-sensitive permeability transition pore. I. Evidence for two separate Me^{2+} binding sites with opposing effects on the pore open probability. J. Biol. Chem. **268**, 1005–1010

56 Bernardi, P. and Petronilli, V. (1996) The permeability transition pore as a mitochondrial calcium release channel: A critical appraisal. J. Bioenerg. Biomembr. **28**, 131–138

57 Brustovetsky, N. and Klingenberg, M. (1996) Mitochondrial ADP/ATP carrier can be reversibly converted into a large channel by Ca^{2+}. Biochemistry, **35**, 8483–8488

58 Kruman, I. I. and Mattson, M. P. (1999) Pivotal role of mitochondrial calcium uptake in neural cell apoptosis and necrosis. J. Neurochem. **72**, 529–540

59 Robb-Gaspers, L. D., Rutter, G. A., Burnett, P., Hajnoczky, G., Denton, R. M. and Thomas, A. P. (1998) Coupling between cytosolic and mitochondrial calcium oscillations: role in the regulation of hepatic metabolism. Biochim. Biophys. Acta **1366**, 17–32

60 Moore W. J. (1972) Electrochemistry: ionics. In Physical Chemistry, p. 444, Prentice-Hall, Englewood Cliffs, NJ, U.S.A.

Received 23 February 2001/3 May 2001; accepted 6 June 2001